Critical Field and Specific Heat in Electron- and Hole-Doped Graphene Superconductors

E.A. Drzazga-Szczęśniak[a,*] and A.Z. Kaczmarek[b]

[a]*Department of Physics, Faculty of Production Engineering and Materials Technology, Częstochowa University of Technology, 19 Armii Krajowej Ave., 42200 Częstochowa, Poland*
[b]*Department of Theoretical Physics, Faculty of Science and Technology, Jan Długosz University in Częstochowa, 13/15 Armii Krajowej Ave., 42200 Częstochowa, Poland*

*e-mail: ewa.drzazga@pcz.pl

Doping is one of the most prominent techniques to alter the properties of a given material. Herein, the influence of the electron- and hole-doping on the selected superconducting properties of graphene are considered. In detail, the Migdal–Eliashberg formalism is employed to analyze the specific heat and the critical magnetic field in the representative cases of graphene doped with nitrogen or boron. It is found that electron doping is much more favorable in terms of enhancing the aforementioned properties than its hole counterpart. These findings are appropriately summarized by means of the dimensionless thermodynamic ratios, familiar in the Bardeen–Cooper–Schrieffer theory. To this end, the perspectives for future research on superconductivity in graphene are drawn.

topics: Eliashberg formalism, critical field, specific heat, superconductivity

1. Introduction

The two-dimensional carbon allotrope known as graphene became one of the most important materials in nanoscience due to its wide range of intriguing properties [1–3]. In particular, much effort has been devoted to the exploration of superconductivity in various graphene-based structures [4–10]. Since superconductivity in pure graphene is absent, doping it with non-carbon elements turned out to be an efficient approach toward the induction of the discussed phase [4–6, 11, 12]. Such promising behavior led to many considerations over recent years. In general, graphene modifications were proposed to induce not only conventional but also unconventional superconductivity [7–10], with the former phase being more anticipated because of its strong theoretical foundations. Strictly speaking, the conventional (phonon-mediated) superconductivity can be induced in graphene by increasing the electron-phonon coupling parameter (λ). This can be done by doping graphene with electrons or holes. A prominent example of such a process is lithium-decorated graphene [4], graphane [5], or nitrogen/boron-doped graphene [6].

In the context of the above developments, nitrogen/boron-doped graphene [6] appears as an exemplary material to study the low-dimensional superconducting phase of interest. This is due to the fact that both of the mentioned materials exhibit relatively high superconducting properties and allow comparing the two doping strategies on the same footing. Therefore, we attempt to investigate the hitherto not discussed thermodynamic properties of the boron- and nitrogen-doped graphene. In particular, we use the Eliashberg formalism to analyze the critical magnetic field and the specific heat. Such analysis is conducted for the 50% nitrogen/boron-doped graphene structure (h-CN/h-CB) under biaxial tensile strain ($\epsilon = 15.6\%/\epsilon = 5\%$) and at the moderate doping level of holes/electrons ($p = 0.4|h|$/unit cell/$n = -0.2|e|$/unit cell) [6]. Our work is organized as follows: in Sect. 2, we describe the theoretical model of the Migdal–Eliashberg equations. Next, in Sect. 3, we discuss the specific heat and related quantities obtained from the numerical analysis of the theoretical model. This study is concluded with a summary and remarks regarding future perspectives in Sect. 4.

2. Theoretical model

In order to describe the thermodynamic properties of the electron- (h-CN) and hole-doped (h-CB) graphene, we adopt the isotropic approximation of the Migdal–Eliashberg equations [13–15]. From the obtained solutions of the Migdal–Eliashberg
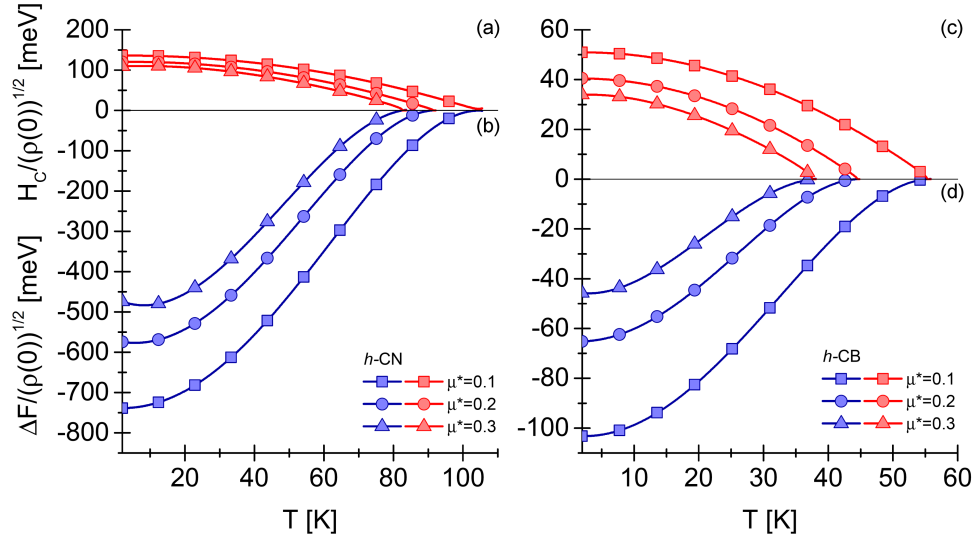
Fig. 1. The free energy difference (panels (b) and (d)) and the critical magnetic field (panels (a) and (c)) as a function of temperature for the selected μ^* values in (a)–(b) the electron- (h-CN) and (c)–(d) hole-doped graphene (h-CB).

equations on the imaginary axis, we are able to determine the order parameter ($\Delta_n = \Delta(i\omega_n)$) with the associated wave function renormalization factor ($Z_n = Z(i\omega_n)$), given as

$$\Delta_n Z_n = \frac{\pi}{\beta} \sum_{m=-M}^{M} \frac{\Delta_m^2}{\sqrt{\omega_m^2 Z_m^2 + \Delta_m^2}}$$
$$\times \left[K\left(i\omega_n - i\omega_m\right) - \mu^\star \theta\left(\omega_c - |\omega_m|\right) \right] \quad (1)$$

and

$$Z_n = 1 + \frac{\pi}{\beta \omega_n} \sum_{m=-M}^{M} \frac{K\left(i\omega_n - i\omega_m\right)}{\sqrt{\omega_m^2 Z_m^2 + \Delta_m^2}} \omega_m Z_m, \quad (2)$$

where $\beta = 1/(k_B T)$ denotes inverse temperature, with k_B being the Boltzmann constant. In what follows, the Matsubara frequency can be written as $\omega_n = (\pi/\beta)(2n-1)$. Moreover, $K(z) = 2\int_0^{\omega_{max}} d(\alpha^2 F(\omega)\omega) \left[(\omega_n - \omega_m)^2 + \omega^2\right]$ and stands for the electron–phonon paring kernel. Note that the $\alpha^2 F(\omega)$ function, conventionally referred to as the Eliashberg function, is adopted from the study of Zhou et al. [6]. Therein, this function was calculated for all cases of interest within the density function theory, as implemented in the Quantum ESPRESSO package. To this end, in (2), the electron–electron depairing interactions are modeled by the Coulomb pseudopotential ($\mu^\star$) parameter, defined as $\mu^\star \equiv \mu^\star \theta(\omega_c - |\omega_m|)$, where θ is the Heaviside function.

The introduced Eliashberg equations are solved here by using the self-consistent iterative procedures developed previously in [16]. The stability of the numerical procedures is reached at around the 2201 Matsubara frequencies, assuming $T_0 = 2$ K and the phonon frequency cut-off (ω_c) equal to $10\omega_{max}$, where $\omega_{max} = 132.6$ meV (h-CN) and

$\omega_{max} = 124.5$ meV (h-CB) and denotes the maximum value of the phonon frequency defined by the adopted $\alpha^2 F(\omega)$ function. Finally, $\mu^\star$ is set to 0.1–0.3, as suggested by Ashcroft [17].

3. Results and discussion

We are starting the description of the selected thermodynamic characteristics by recalling the free energy difference between the normal and superconducting state (ΔF)

$$\frac{\Delta F}{\rho(0)} = -\frac{2\pi}{\beta} \sum_{m=1}^{M} \left(\sqrt{\omega_m^2 + \Delta_m^2} - |\omega_m| \right)$$
$$\times \left(Z_m^S - \frac{|\omega_m|}{\sqrt{\omega_m^2 + \Delta_m^2}} Z_m^N \right), \quad (3)$$

with the renormalization factors Z_m^S and Z_m^N for the superconducting (S) and normal (N) state. In panels (b) and (d) in Fig. 1, we have presented the dependence of the $\Delta F/\rho(0)$ on the temperature for both considered structures. We remark that the negative values of the considered function confirm the thermodynamic stability of the superconducting phase for the h-CN (a, b) and h-CB (c, d). Moreover, it is observed that the increase of the Coulomb pseudopotential leads to the decrease of the $\Delta F(0)$ parameter, since

$$\frac{\left[\Delta F(0)\right]_{\mu^*=0.3}}{\left[\Delta F(0)\right]_{\mu^*=0.1}} \approx 0.63 \quad (4)$$

and

$$\frac{\left[\Delta F(0)\right]_{\mu^*=0.3}}{\left[\Delta F(0)\right]_{\mu^*=0.1}} \approx 0.44, \quad (5)$$
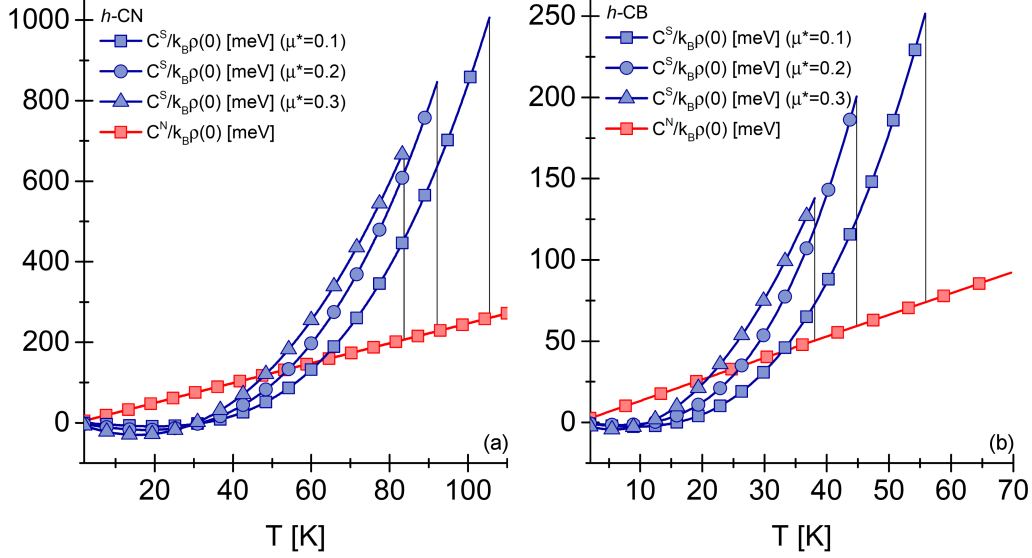
Fig. 2. The specific heat for the superconducting and normal state as a function of the temperature for the selected μ^* values in (a) the electron- (h-CN) and (b) hole-doped graphene (h-CB). The specific heat jump at the critical temperature is marked by the solid vertical line.

for h-CN and h-CB, respectively (assuming $F(0) = F(T_0)$). Clearly, the free energy difference for the boron-doped graphene is less robust towards an increase of μ^*. Next, by using the $\Delta F/\rho(0)$ function, the magnetic critical field can be obtained from the formula

$$\frac{H_C}{\sqrt{\rho(0)}} = \sqrt{(-8\pi)\frac{\Delta F}{\rho(0)}}. \qquad (6)$$

The panels (a) and (c) in Fig. 1 represent the thermal behavior of the critical magnetic field for the selected values of the parameter μ^*. It can be observed that the $H_C/\sqrt{\rho(0)}$ function decreases with the increase in temperature. Moreover, the value of the critical field strongly diminishes upon the increase of the Coulomb pseudopotential. This fact can be seen from the ratios obtained for the electron- and hole-doping case, respectively,

$$\frac{\left[H_C(T_0)\right]_{\mu^*=0.3}}{\left[H_C(T_0)\right]_{\mu^*=0.1}} \approx 0.8 \qquad (7)$$

and

$$\frac{\left[H_C(T_0)\right]_{\mu^*=0.3}}{\left[H_C(T_0)\right]_{\mu^*=0.1}} \approx 0.66. \qquad (8)$$

From the values of these ratios, one can conclude that the superconducting state for the h-CN is more stable under the change of the Coulomb pseudopotential.

Accordingly, the thermal characteristics of the superconducting phase C^S from the difference in the specific heat between the superconducting and normal state ($\Delta C = C^S - C^N$) takes form

$$\frac{\Delta C}{k_B\rho(0)} = -\frac{1}{\beta}\frac{d^2\left|\Delta F/\rho(0)\right|}{d(k_BT)^2}, \qquad (9)$$

where the specific heat of the normal state has been obtained from the formula

$$\frac{C^N}{k_B\rho(0)} = \frac{\gamma}{\beta}, \qquad (10)$$

with the Sommerfeld constant given as $\gamma \equiv \frac{2\pi^2}{3}(1+\lambda)$. The detailed derivation of (9) and (10) can be seen in [15, 18]. In Fig. 2, we have presented the thermal behavior of the specific heat C^N and C^S for the h-CN and h-CB materials, respectively. Both functions increase with the increase in temperature: for the superconducting state, C^S changes exponentially at low temperatures, while for the normal state, the increase of the values is linear. Moreover, the specific heat of the superconducting phase is also affected by the increase of the Coulomb pseudopotential, as can be seen from the analysis for $\mu^* \in \{0.1, 0.2, 0.3\}$. Is it worth noting that a characteristic jump in the C^S occurs for $T = T_C$, and the value of the specific heat jump is lowered by the depairing electron correlations in the h-CN and h-CB structures. In fact,

$$\frac{\left[\Delta C(T_C)\right]_{\mu^*=0.3}}{\left[\Delta C(T_C)\right]_{\mu^*=0.1}} \approx 0.67 \qquad (11)$$

and

$$\frac{\left[\Delta C(T_C)\right]_{\mu^*=0.3}}{\left[\Delta C(T_C)\right]_{\mu^*=0.1}} \approx 0.55 \qquad (12)$$

for the electron- and hole-doped graphene, respectively. It is important to notice that the described behavior matches the expected characteristics for phonon-mediated superconductivity, as stated in [15]. Hence, it can be stated that the results presented in Figs. 1 and 2 are consistent with the electron-phonon pairing mechanism of the discussed graphene structures.

TABLE I

Values of the thermodynamic parameters of the superconducting state for the h-CN and h-CB.

	h-CN	h-CB
λ	3.35	1.34
$\omega_{\max}$ [meV]	132.6	124.5
ω_c [meV]	$10\omega_{\max}$	$10\omega_{\max}$
$\mu^\star$	$\langle 0.1, 0.2, 0.3 \rangle$	$\langle 0.1, 0.2, 0.3 \rangle$
T_C [K]	$\langle 105.6, 92.2, 83.8 \rangle$	$\langle 55.9, 44.9, 38.1 \rangle$
$2\Delta(0)$ [meV]	$\langle 47.95, 41.36, 37.22 \rangle$	$\langle 20.59, 16.09, 13.43 \rangle$
R_Δ	$\langle 5.27, 5.21, 5.16 \rangle$	$\langle 4.27, 4.16, 4.09 \rangle$
R_C	$\langle 2.87, 2.72, 2.28 \rangle$	$\langle 2.41, 2.39, 1.74 \rangle$
R_H	$\langle 0.128, 0.125, 0.125 \rangle$	$\langle 0.138, 0.140, 0.144 \rangle$

To this end, we note that our previous analysis allows us to calculate the dimensionless thermodynamic parameters:

$$R_H = \frac{T_C \, C^N(T_C)}{H_C^2}, \qquad R_C = \frac{\Delta C(T_C)}{C^N(T_C)}, \tag{13}$$

and

$$R_\Delta = \frac{2\Delta(0)}{k_B T_C},$$

values of which are presented in Table I. The estimated values are different from their counterparts obtained within the Bardeen–Cooper–Schrieffer (BCS) theory: $[R_H]_{\mathrm{BCS}} = 0.168$, $[R_C]_{\mathrm{BCS}} = 1.43$, and $[R_\Delta]_{\mathrm{BCS}} = 3.53$ [19, 20]. Therefore, the analysis presented here suggests the pivotal role of the retardation and strong coupling effects in the considered graphene structures.

4. Conclusions

In this work, we have extended previous investigations of the superconducting state in the h-CN and h-CB allotropes, initiated originally in [6], based on the combination of the density functional theory and the Allen–Dynes modified McMillan formula [21]. Herein, we have conducted the analysis within the Migdal–Eliashberg formalism in order to account for the strong-coupling and phonon-mediated character of the superconducting phase in these graphene structures. In this manner, the presented study complements not only the work by Zhou et al. [6] but also our previous investigations of the conventional superconductivity in graphene- [11, 12, 22, 23] or generally carbon-based structures [24–26]. This is to say that the presented discussion constitutes a contribution to the wider research domain aimed at the search for a strong conventional superconducting phase in low-dimensional carbon structures.

To be specific, the presented analysis involved a description of the thermodynamic critical field, the free energy difference, and the specific heat for the superconducting state in both scenarios. In order to be as general as possible, our analysis has been performed for the three different values of the Coulomb pseudopotential $\mu^* \in \{0.1, 0.2, 0.3\}$. It was shown that doping graphene with electrons seems to be more favorable in terms of enhancing its superconducting properties than in the case of the hole-doping procedure. Our analysis also confirmed the strong-coupling behavior of the considered materials. The dimensionless ratios (R_Δ, R_C, R_H), as presented in Table I, clearly reinforce this statement since each one of them notably exceeds the limits of the Bardeen–Cooper–Schrieffer theory [19, 20]. This is due to the fact that Eliashberg equations are considered to provide quantitative rather than qualitative results for the strong-coupling superconductors ($\lambda > 0.5$) [15, 27]. Such quantitative elucidation is somewhat confirmed by the T_C values obtained within the Eliashberg formalism (again, see Table I), which are predicted to be higher than the values calculated based on the Allen–Dynes modified McMillan formula, as shown in [6]. Note that such a trend was observed previously in terms of other strong-coupling and phonon-mediated superconductors, with the related Eliashberg estimates being in close agreement with the experimental predictions (see, e.g., studies on $Ba_{1-x}K_xBiO_3$ [28] or Pb [29]).

References

[1] K.S. Novoselov, A.K. Geim, S.V. Morozov, D. Jiang, Y. Zhang, S.V. Dubonos, I.V. Grigorieva, A.A. Firsov, *Science* **306**, 666 (2004).

[2] A. Das, S. Pisana, B. Chakraborty, S. Piscanec, S.K. Saha, U.V. Waghmare, K.S. Novoselov, H.R. Krishnamurthy, A.K. Geim, A.C. Ferrari, A.K. Sood, *Nat. Nanotech.* **3**, 210 (2008).

[3] J. Ye, S. Inoue, K. Kobayashi, Y. Kasahara, H.T. Yuan, H. Shimotani, Y. Iwasa, *Nat. Mater.* **9**, 125 (2010).

[4] G. Profeta, M. Calandra, F. Mauri, *Nat. Phys.* **8**, 131 (2012).

[5] G. Savini, A.C. Ferrari, F. Giustino, *Phys. Rev. Lett.* **105**, 037002 (2010).

[6] J. Zhou, Q. Sun, Q. Wang, P. Jena, *Phys. Rev. B* **92**, 064505 (2015).

[7] A.M. Black-Schaffer, S. Doniach, *Phys. Rev. B* **75**, 134512 (2007).

[8] M.L. Kiesel, C. Platt, W. Hanke, D. Abanin, R. Thomale, *Phys. Rev. B* **86**, 020507 (2012).

[9] T. Ma, F. Yang, H. Yao, H.-Q. Lin, *Phys. Rev. B* **90**, 245114 (2014).

[10] B.M. Ludbrook, G. Levy, P. Nigge et al., *PNAS* **112**, 11795 (2015).

[11] D. Szczęśniak, R. Szczęśniak, *Phys. Rev. B* **99**, 224512 (2019).

[12] D. Szczęśniak, E.A. Drzazga-Szczęśniak, *Eur. Phys. Lett.* **135**, 67002 (2021).

[13] A.B. Migdal, *Sov. Phys. JETP* **34**, 996 (1958).

[14] G.M. Eliashberg, *Sov. Phys. JETP* **11**, 696 (1960).

[15] J.P. Carbotte, *Rev. Mod. Phys.* **62**, 1027 (1990).

[16] R. Szczęśniak, *Acta Phys. Pol. A* **109**, 179 (2006).

[17] N. Ashcroft, *Phys. Rev. Lett.* **92**, 187002 (2004).

[18] J. Blezius, J.P. Carbotte, *Phys. Rev. B* **36**, 3622 (1987).

[19] J. Bardeen, L.N. Cooper, J.R. Schrieffer, *Phys. Rev.* **106**, 162 (1957).

[20] J. Bardeen, L.N. Cooper, J.R. Schrieffer, *Phys. Rev.* **108**, 1175 (1957).

[21] P.B. Allen, R.C. Dynes, *Phys. Rev. B* **12**, 905 (1975).

[22] D. Szczęśniak, A.P. Durajski, R. Szczęśniak, *J. Phys. Condens. Matter* **26**, 255701 (2014).

[23] D. Szczęśniak, *Eur. Phys. Lett.* **111**, 18003 (2015).

[24] R. Szczęśniak, E.A. Drzazga, D. Szczęśniak, *Eur. Phys. J. B* **88**, 52 (2015).

[25] E.A. Drzazga, I.A. Wrona, R. Szczęśniak, *Mod. Phys. Lett. B* **33**, 1950089 (2019).

[26] E.A. Drzazga, A.M. Duda, R. Szczęśniak, *Physica B* **445**, 68 (2014).

[27] M. Cyrot, D. Pavuna, *Introduction to Superconductivity and High-TC Materials*, World Scientific, Singapore 1992.

[28] D. Szczęśniak, A.Z. Kaczmarek, E.A. Drzazga-Szczęśniak, R. Szczęśniak, *Phys. Rev. B* **104**, 094501 (2021).

[29] R. Szczęśniak, *Solid State Commun.* **144**, 27 (2007).